PARAMETERS FOR STUDY 2

Version 2

**R.B. Palmer, S. Berg, R. Fernow, Y. Fukui,
J Gallardo, C. Kim, E. Kim, H. Kirk, J. Miller,
N. Mokhov, G. Penn, R. Weggel, J. Wurtele**

1/16/01

Abstract

The parameters are given for the front end of a neutrino factory. No RF is employed near the target and relatively little polarization (22 %) is achieved, but the efficiency of producing muons is good (≈ 0.18 μ/p with 24 GeV proton bunches with 3 ns rms length). Per MW of proton power, this is 6.6 $\times$ the performance of Feasibility Study 1.

The high efficiency is achieved by

1) using a liquid mercury target;

2) using three induction linacs and long drifts to achieve near non-distorting phase rotation into a longer bunch train with less momentum spread; and

3) tapering the focus strength in the cooling system so that the angular spread of the muons being cooled is maintained at a near constant value.

Contents

1 Introduction

This note gives specifications and some simulation results for Feasibility Study 2 neutrino factory.

This document can be found at:
http://pubweb.bnl.gov/people/palmer/nu/study2/params.ps
and the tex files that made it at:
http://pubweb.bnl.gov/people/palmer/nu/study2/tex

The scheme is illustrated in the following figure:

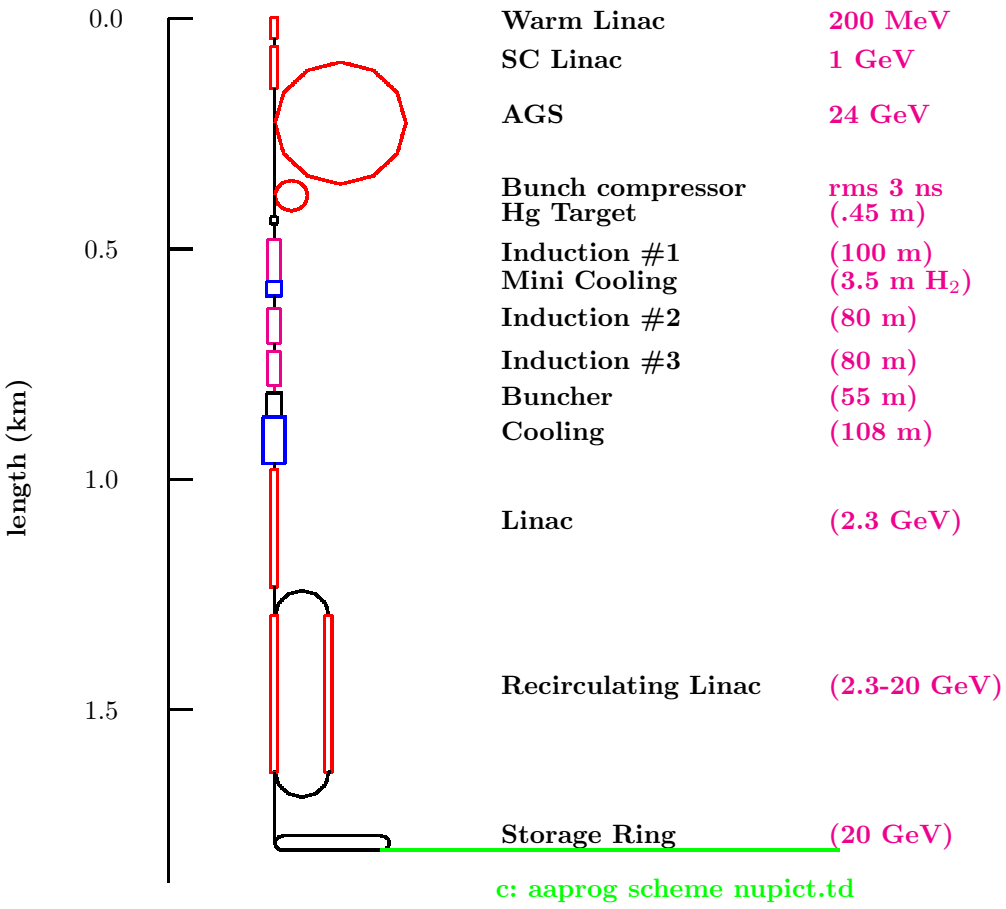

The axial field is 20 T at the target and tapers down to 1.25 T over 18 m. The field is reversed between the two halves of the hydrogen "mini-cooling" absorber at about 150 m. At 370 m there is a match from the -1.25 T fixed field to a Super FOFO lattice consisting of 2.75 m cells. There is another match at 480 m to a shorter cell (1.65 m).

The lengths of the main components are listed in the following table:

	length m	totals m
target	0.45	0
taper	17.6	17.6
drift	18	35.6
Induction 1	100	135.6
Drift	5	140.6
Mini-Cool	10	150.6
Drift	35	185.6
Induction 2	80	265.6
Drift	20	285.6
Induction 3	80	365.6
Match to Super FOFO	17.5	383.1
Buncher	$20 \times 2.75 = 55$	428.1
cooling part 1	$16 \times 2.75 = 44$	472.1
match	4.4	476.5
cooling part 2	$36 \times 1.65 = 59.4$	535.9
Linac	275	
RLA arcs	270	
RLA Linacs	2×366	
Storage Ring Arcs	2×53	
Storage ring Straights	2×216	

2 Specifications

2.1 Proton driver

Energy	24	GeV
protons per bunch	$\approx 1.7 \ \ 10^{13}$	
bunches per fill	6	
time between extracted bunches	≈ 20	ms
repetition rate	2.5	Hz
rms bunch length	≤ 3	ns
beam power	≥ 1	MW
normalized emittance (95%)	mm mrad	100
normalized emittance (rms)	mm mrad	17

Finite time between bunches is required for a number of reasons:

- To allow time to refill the RF cavities in the accelerating systems and avoid excessive beam loading;
- To avoid the need for multi pulsing of the induction linacs; and
- to allow the liquid target to be re-established after its assumed dispersal by the previous bunch. It is this requirement that sets the minimum spacing: The time required depends on the jet velocity and other parameters, and is not yet known. The number of 20 ms is a reasonable starting assumption. An even separation of bunches at 15 Hz would also be even better, but would require an accumulator ring.

The possibility of an average power greater than 1 MW, up to 1.5 MW should also be considered. This would correspond to the average power assumed in Feasibility Study 1.

Lengths or circumferences of the major components are given below

	len m	ΔE GeV	f MHz
Conventional linac	150	0.2	200
SC linac	55	.2-.7	??
SC linac	88	.7-1.5	??
AGS synchrotron	807	1.5-24	??
Fixed field buncher ring	202	24	??

2.2 Target

A single proton bunch will heat the liquid to a temperature above its boiling point and generate substantial shock pressures. It is not believed that these will have significant adverse consequences, but, if it did, liquid lead/tin eutectic could be used. A graphite target (as used in study 1) could also be considered as a backup, but would reduce the neutrino intensity by a factor of 1.9 (see section 3.5).

In the Study 2 target system, the beam with rms radius σ_r intersects a mercury jet of radius r_o at an angle $\theta_{crossing}$. The forward velocity of the jet is v_o. The intervals between pulses is t, and it will be assumed here that after a pulse, all the mercury outside of the nozzle is dispersed. The nozzle is at z_{nozzel} with respect to the intersection of the beam and jet center lines. Consider the following parameters:

length	30	cm
displacement of front from axis	≈ 1	cm

beam σ_r	1.5	mm
beam angle to magnet axis	100	mrad
jet material	mercury	
velocity	20-30	m/sec
jet r_o	5	mm
$\theta_{crossing}$	33	mrad
t between bunches	20	ms
nozzel to magnet center	37.5	cm

The distribution of resulting interactions as a function of z is shown above. At the time of a second, or subsequent bunch, the newly established jet will extend a distance $z_{jet} = v_o\ t = 0.6$ m from the nozzle. It is seen that only 2.5 % of the interactions would occur after this location, had the beam extended indefinitely. Thus there is a negligible loss from this limited jet extent.

Thus the total length over which the jet must propagate without serious magnetic disruption is from the nozzle to a point 0.6 m downstream. In order to minimize the field non uniformity over this length, the magnetic center (approximate point of maximum B_z is placed at the center of this length. i.e. the magnetic center is set at a distance $z_{magnet} = z_{jet}/2 - z_{nozzel} = \ -.15$ m with respect to the jet-beam intersection. the figures shown here use a horizontal scale with $z = 0$ at the magnetic center.

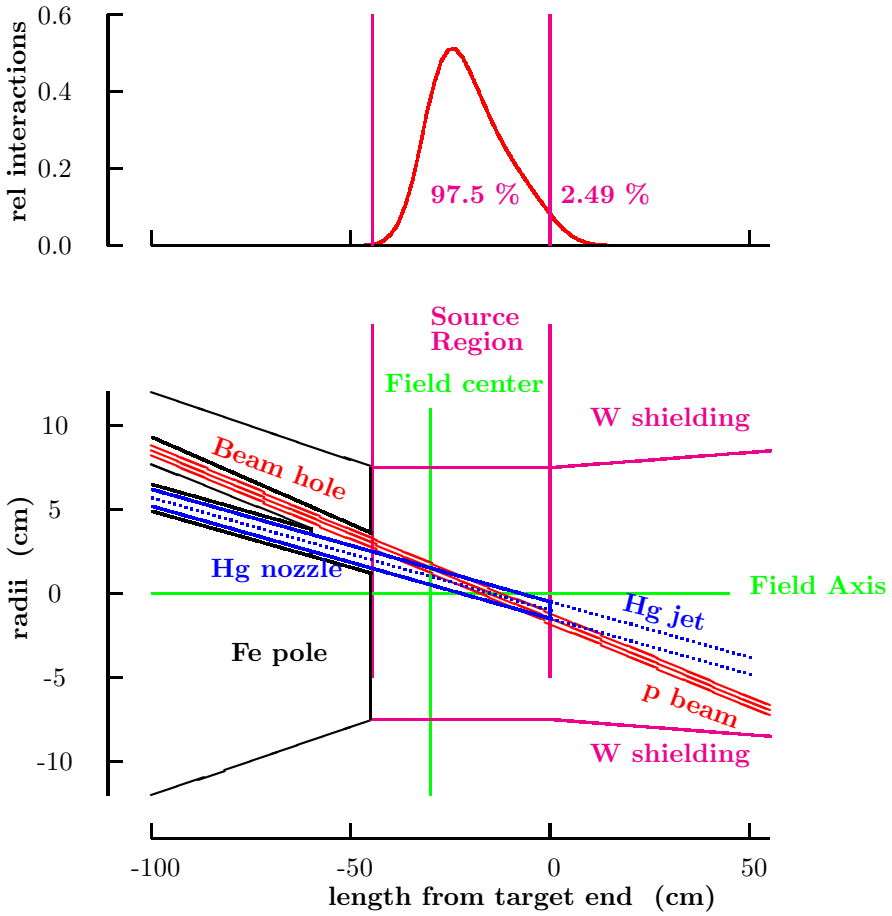

The layout is shown above. The proton beam enters at an angle θ_{beam} with respect to the magnet axis. The jet is at an angle $\theta_{jet} = \theta_{beam} - \theta_{crossing}$. The vertical distance y_o from the magnet center $(z = 0, r = 0)$ to the jet axis at $z = 0$ can be chosen to minimize beam disruption. We assuming a Gaussian distribution of B'_z vs z', with a maximum value of B_o, The jet conductivity κ, density ρ, and surface tension $T_{surface}$, and the other parameters are given below:

B_o	20	T
σ'_z	.8	m
θ_{jet}	-67	mrad
y_o (without surface tension)	2	mm
y_o (with surface tension)	1	mm
κ	10^6	Ω m
ρ	13.5 10^4	kg/m^3
T_{surface}	.456	N/m
$p_{\text{gas}} = p_{\text{atmospheric}}$	10^5	N/m^2

Perturbation calculations (see ref***) show that over the extent of the new jet (from - .3 to .3 m):

- The maximum axial field deviations are +/− 1.25 T = 6%
- The transverse fields seen by the jet are approximately 1.4 T, and vary at the ends by only up to +/− 0.01 T = +/− 0.7 %. But it is this small variation of transverse field that generate axial current in the jet, leading to jet shape distortions that are the most serious constraint on the magnet design.
- The axial pressure difference has a minimum of - 0.5 atmospheres. Thus if the jet is operating in a gas (He or Argon) at a pressure of 1 atmosphere, then the minimum pressure will be + 0.5 atmospheres, and there will be no tendency to cavitate prior to the arrival of the beam.
- The maximum average deceleration of the jet is small compared to the average jet velocity: 0.11/30≈0.3%.
- The maximum decelerations (from shear forces) are also small compared to the average jet velocity: 0.7/30≈2.3%.
- The deflections of the jet are very small: 20 μm.
- The resulting calculated jet distortions (Δ width / ave width) with no jet axis displacement ($y_o = 0$) are approximately 30% without surface tension, but are reduced to 10%, by the restraint from surface tension. Both can be reduced to 6-7% by small jet axis displacements.

These disruptions are all relatively small, and should, with the fields assumed, cause no problems. However, relatively small field changes can make the beam distortions uncomfortably large. It thus appears that considerations of these distortions will set the tolerances on the magnetic field shape. Tuning of these distortions can be achieved by vertical displacements of the jet, and provision for mechanically adjusting this should be considered.

2.3 Beam Transport and field reversal

2.3.1 Capture and matching Solenoids

The 20 T capture solenoid would be a hybrid, with copper (insert) and superconducting (outsert), magnet similar to that discussed in Feasibility Study 1. However, it is proposed here to use hollow copper conductor for the insert, rather than a Bitter style magnet in Study 1. The choice is aimed at achieving longer magnet life and avoiding any problems with highly irradiated water insulation. It is understood that the initial cost will be higher.

After the 20 T magnet, coils are designed to taper the axial field down slowly to 1.25 T over a distance of approximately 18 m. The form of the tapered field is approximately:

$$B(z) \approx \frac{20}{1 + k\, z}$$

Dimensions of coils that achieve this taper are given in the following table: The final design will have to include space for the beam dump and shielding.

These coils, and their axial field profile, are shown in the following figures:

2.3.2 Beam Transport

After the solenoid taper, the beam is transported through drifts, the phase rotation linacs, and the mini-cooling hydrogen absorbers, in a transport channel consisting of solenoid coils with a 50 cm periodicty. The coil radii are larger at the beginning to allow space for shielding.

length	18-48	48-148	148-368	m
bore radius	30	30	30	cm
coil IR	38	33	32.5	cm
coil thickness	.8-1	.8-1	.8-1	cm
axial field	1.25	1.25	1.25	T
coil periodicity	50	50	50	cm
coil lengths	36	36	36	cm

2.3.3 Field Reversal

Between the two hydrogen absorbers, there is a 10 m long chromatically matched field reversal. This reversal in needed for two reasons:

- between two halves of the absorber, it is needed to avoid generating finite canonical angular momentum from the reduction of angular momentum in the absorbers; and
- at some point along the phase rotation a field reversal is needed to avoid generating a correlation between the canonical angular momenta of individual tracks and their energy after correction by the induction units.

By serendipity, a single flip appears to meet both requirements.

The field reversal was designed to match β's from start to end, over a momentum bite of 200 +/− 90 MeV. The coils used in the optimization were larger than needed and had very low current densities. More reasonable coils will be relatively easy to design, but it has not yet been done. We thus specify the reversal by the required axial fields:

length m	Field T
.000	-1.25
.2655	-1.2446
.5309	-1.2242
.7963	-1.1874
1.0617	-1.1357
1.3271	-1.0852
1.5925	-1.0664
1.8579	-1.0801
2.1233	-1.0661
2.3887	-.97434
2.6541	-.84339
2.9195	-.76098
3.1849	-.78458
3.4503	-.9125
3.7157	-1.0631
3.9811	-1.0747
4.2465	-.81469
4.5119	-.30422
4.7773	.30242

continued

5.0427	.81346
5.3081	1.0744
5.5735	1.0635
5.8389	.913
6.1043	.78483
6.3697	.76088
6.6351	.84302
6.9005	.97396
7.1659	1.0659
7.4313	1.0802
7.6967	1.0664
7.9621	1.0851
8.2275	1.1355
8.4929	1.1873
8.7583	1.2241
9.0237	1.2445
9.2891	1.251
10.0	1.25

These axial fields are plotted in the following figure, together with the β's obtained for a set of different momenta.

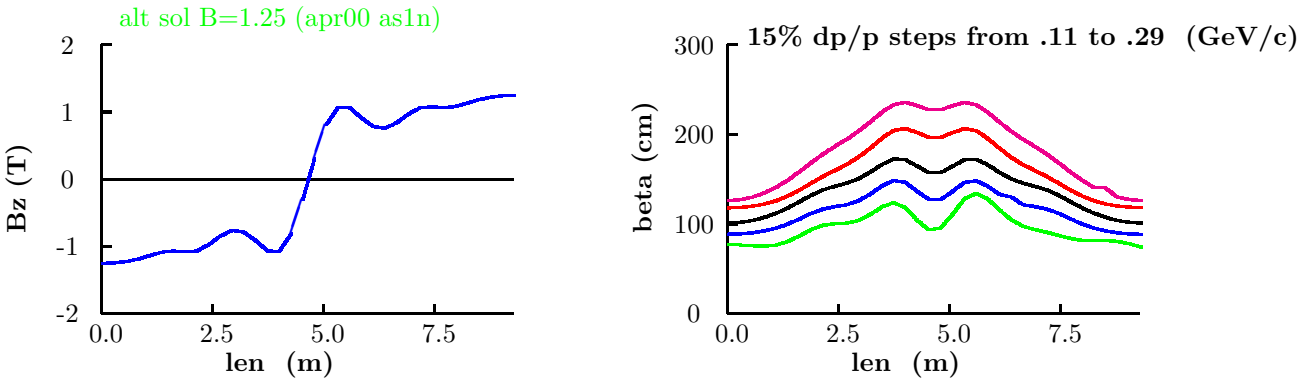

2.4 Phase Rotation

2.4.1 Introduction

Induction linacs combined with drifts and hysrogen absorbers are used to 'phase rotate' the beam. After a drift, low energy particles which fall back in the bunch are accelerated, while the high energy particles which remain in the fron tof the bunch are decellerated. As a result, a distribution that has an initially large energy spread, but short time spread, is rotated into a bunch with small energy spread but long time spread. If the process is done with a single drift and single induction linac, then relativistic effects cause a distortion of the rotated bunch such that the initially high energy particles end with a larger energy spread than the initially low energy ones. The use of two induction linacs, with a drift between them allows this distortion to be greatly reduced.

A hydrogen absorber is used after the first induction linac to reduce the beam energy, allowing the first linac to be unipolar, and to reduce the emittance. This "mini-cooling' absorber is in two parts with the field reversal between them.

2.4.2 Induction Linacs

A first linac is introduced close to the taqrget and forms the time energy distribution to give non-distorting phase rotation later. The second and third induction linacs were initially combined in a single bipolar induction linac, but have been separated for economic reasons. The performance was not changed by this change.

		1	2	3
length	m	100	80	80
inner radius	cm	30	30	30
Solenoid field	T	1.25	1.25	1.25
maximum gradient	MV/m	1.55	1.45	1.0
pulse length	nsec	190	100	360

The shape of the accelerating pulse is given in the following tables and plots:

Ind	1
t	G
nsec	MV/m
5	0.0
15	29.1
30	65.9
50	93.8
90	123.3
130	139.4
170	155.0
190	135.0
200	50.0
220	0.0

Ind	2
t	G
nsec	MV/m
-34	0.0
-24	-145.0
-14	-145.0
-4	-118.8
6	-70.0
16	-53.1
26	-37.5
36	-28.1
46	-21.3
56	-15.6
66	-10.6
76	-6.3
86	-3.1
96	-1.3
106	0.0

Ind	3
t	G
nsec	MV/m
-15	0.0
10	7.5
35	32.5
60	48.8
85	63.8
110	70.0
135	78.1
160	82.5
185	90.0
210	96.3
235	99.4
260	100.0
285	100.0
310	100.0
335	100.0
360	62.5
385	0.0

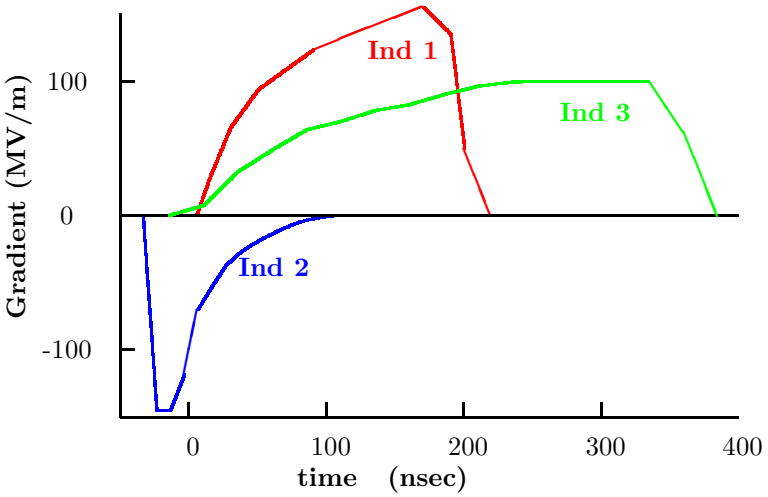

2.4.3 Mini-cooling Hydrogen absorbers

Between the first and second induction linacs, hydrogen is introduced to lower the energies and reduce the transverse emittance. The hydrogen is divided into two parts (1.75 m long each) with a chromatically matched field reversal between them.

At the front of the first hydrogen absorber there is a thick cooled room temperature Be absorber to take the energy from low energy particles in the beam pipe and avoid excessive heating of the hydrogen.

Be thickness	??	cm
first hydrogen length	1.75??	m
second hydrogen length	1.75	m
hydrogen radius	30	cm

2.5 Match form solenoid to super FOFO lattice

A match is required between the approximately uniform 1.25 T solenoid fields in the previous sections, and the super FOFO lattices used in the following. This match should be chromatically matched, but since the momentum spread is relatively small (≈ 4 % rms), the chromatic correction is less critical than, for instance, in the field reversal.

The following table gives coil dimensions and current densities for the match. The current densities given here are lower than used in the following lattice and should be increased here too, to minimize their cost.

len1 m	dl m	rad m	dr m		I/A A/mm^2
0.000	1.375	0.300	0.100	2	-9.99
1.375	1.375	0.300	0.100	2	-9.99
2.750	1.375	0.300	0.100	2	-9.99
4.125	1.375	0.300	0.100	2	-9.99
5.500	1.375	0.300	0.100	2	-9.99
6.875	1.375	0.300	0.100	2	-9.99
8.250	0.330	0.300	0.110	2	-15.57
8.949	0.187	0.330	0.330	6	-33.40
9.466	0.187	0.330	0.330	6	35.19
10.511	0.330	0.770	0.110	2	66.12
11.665	0.187	0.330	0.330	6	43.75
12.182	0.187	0.330	0.330	6	-43.75
13.227	0.330	0.770	0.110	2	-67.40
14.415	0.187	0.330	0.330	6	-43.75
14.932	0.187	0.330	0.330	6	43.75
15.977	0.330	0.770	0.110	2	66.12
17.165	0.187	0.330	0.330	6	43.75

The coils, their fields, and the β's for three different momenta are plotted in the following figure:

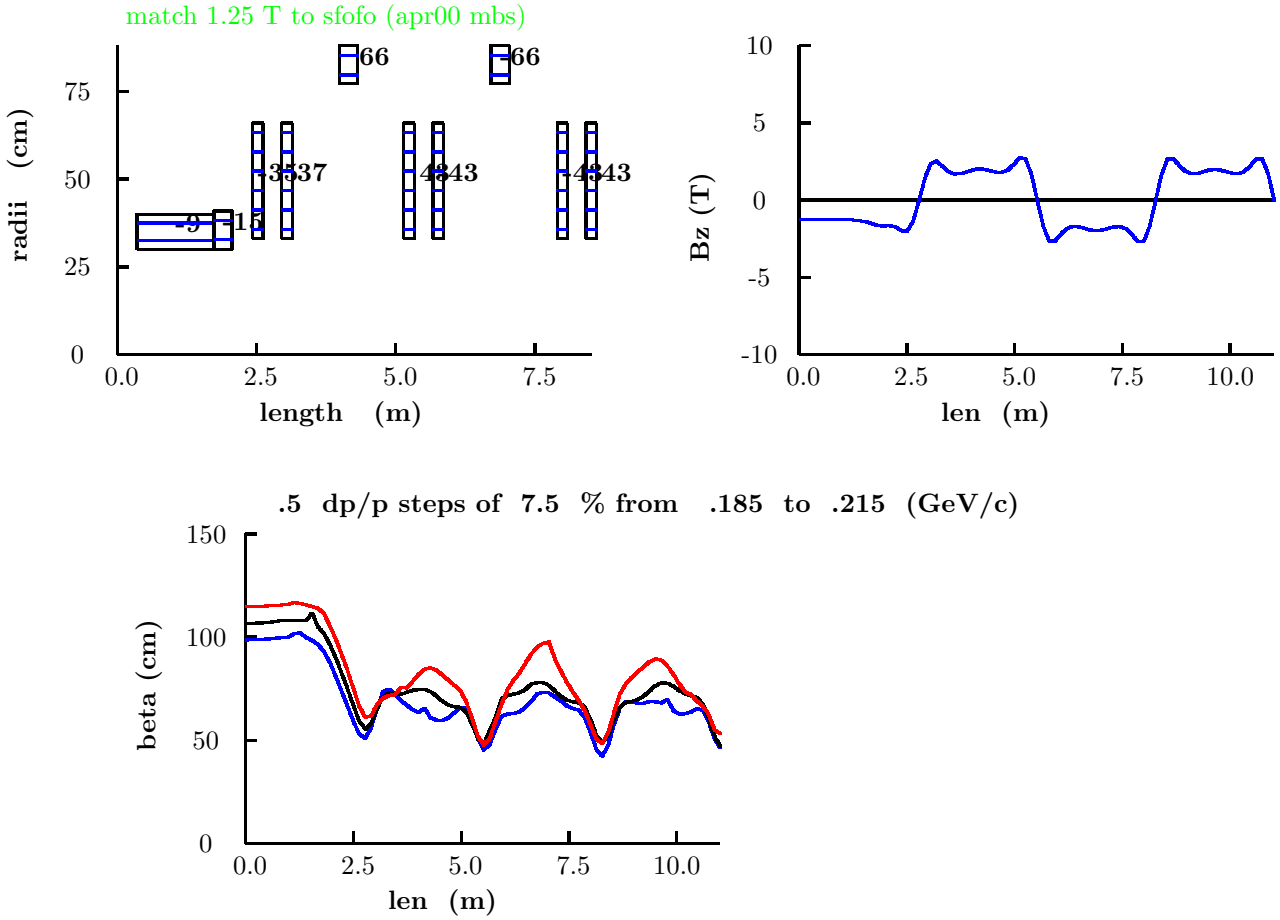

It is seen that the match is not very good, although there appear to be little adverse consequences.

The apertures in this matching section were set wide open and have not yet been optimized.

2.6 Buncher

The bunching is done in the same lattice as used for the first cooling stage (1,1), which is described in section 2.11. A total of 20 cells are used, giving it a length of $20 \times 2.75 = 55$ m.

The buncher consists of three stages:

1. low field 200 MHz rf with 400 MHz harmonic, followed by a long drift (27.5 m)

2. medium field 200 MHz rf with 400 MHz harmonic, followed by a shorter drift (11 m)

3. higher field 200 MHz rf followed by a short drift (5.5 m)

2.6.1 RF

The locations and lengths of the RF components are listed in the following table:

	len m	freq MHz	grad Mv/m
harmonic rf	.186	402.5	6.4
space	.443		
rf	4 × .373	201.25	6.4
space	.443		
harmonic rf	.186	402.5	6.4
drift 1	10 × 2.75		
harmonic rf	.186	402.5	6
space	.443		
rf	4 × .373	201.25	6
space	.443		
harmonic rf	2 × .186	402.5	6
space	.443		
rf	4 × .373	201.25	6
space	.443		
harmonic rf	.186	402.5	6
drift 2	3 × 2.75		
space	.629		
rf	4 × .373	201.25	8
space	.629		
space	.629		
rf	4 × .373	201.25	8
space	.629		
drift 3	2 × 2.75		

2.6.2 RF window radii and thicknesses

	rad m	thickness μm
windows at ends of each 400 MHz cavity	.2	100
windows at end of each set of 4 200 MHz cavities	.21	125
windows between the 4 400 MHz cavities	.25	250

2.7 Cooling Latices

2.7.1 Introduction

The cooling is done in six sections with steadily decreasing β's. This is done to maximize the cooling rate. Too small a β at a given emittance results in too large divergence angles and particle loss. Too large a β gives small divergence angles and a greater relative emittance growth from coulomb scattering. The best β scales down with the emittance and is always such as to give a certain constant divergence angles ($\sigma_{x'} = \sigma_{y'} \approx 0.1$).

The six sections are made from two different physical lattices [(1) and (2)], with three different current setting in each: 1,1 1,2 1,3 in the first lattice, and 2,1 2,2 2,3, in the second. The final cooling section (2,3) is further broken into 2 parts (2,3a) and (2,3b) that differ only in their window sizes and thicknesses.

The lengths of the sections are:

	length m	total length m
cool 1,1	$4 \times 2.75 = 11$	11
match 1,1-2	$2 \times 2.75 = 5.5$	16.5
cool 1,2	$4 \times 2.75 = 11$	27.5
match 1,2-3	$2 \times 2.75 = 5.5$	33
cool 1,3	$4 \times 2.75 = 16.5$	49.5
match 1,3-2,1	4.4	53.9
cool 2,1	$12 \times 1.65 = 19.8$	73.7
match 2,1-2	$2 \times 1.65 = 3.3$	77
cool 2,2	$8 \times 1.65 = 13.2$	90.2
match 2,2-3	$2 \times 1.65 = 3.3$	93.5
cool 2,3	$12 \times 1.65 = 19.8$	113.3

The lattices used have been named "Super FOFO". The "FOFO" refers to the basic sequence of alternating solenoids, that focus the beam and generate β, and thus beam size, minima between the solenoids. The "Super" part, proposed by A. Sessler, is the replacement of the simple alternating solenoids with alternating, but more complex, solenoid systems. In this case the systems consist of strong short "focusing" solenoids at either end, and a weaker "coupling" fields between them.

An example of the fields (for the last part) is given below

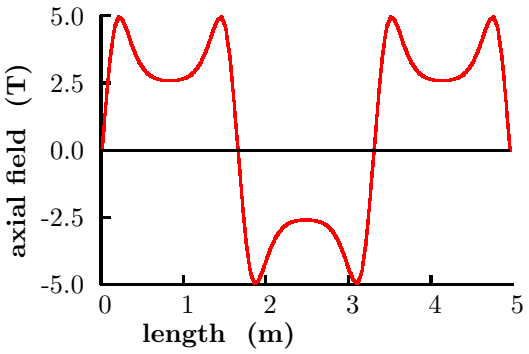

The following figure shows the beta's, as a function of momentum, for the six cases.

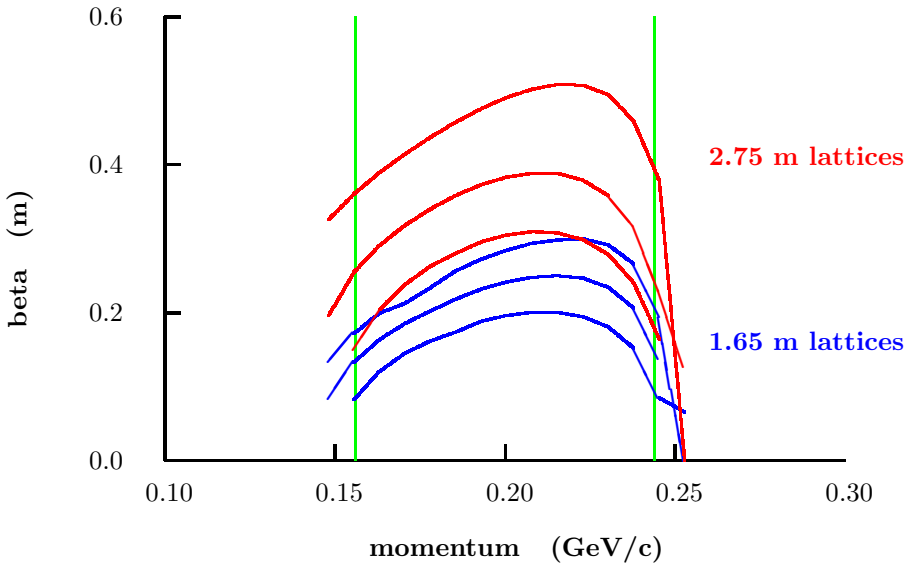

In all cases the β functions are seen to have sharp drops above and below the required momentum acceptance. These are due to the approach to two resonances. At the lower momentum it corresponds to a 2 π phase advance per cell, and at the higher momentum to 1 π phase advance. With any given lattice length, the central beta and its location can be controlled by adjusting two characteristics, or parameters, of the focusing fields. The details of the fields

are not important, just these two characteristics:

- the strength of the opposed "focusing" fields near the lattice ends (the higher the fields, the higher the momentums focused)
- the general magnitude of the field in the central part of the lattice (a higher "coupling" field reduces the end betas, but increases the momentum acceptance)

By adjusting these two characteristics, we can keep the betas symmetric about the required mean momentum, and independently reduce the central beta value. But as we decrease the coupling fields, the momentum acceptance shrinks and, at some point, becomes unacceptably small. At this point we are forced to use a shorter lattice which, though it will require higher fields, allows the betas to be further reduced while again achieving adequate momentum acceptance and keeping the betas symmetric.

The two characteristics can be obtained in a number of different ways. The required lattice performance can, for instance, be obtained by having only a pair of oppositely driven short solenoids on either side of each absorber. The two parameters to be controlled, in this case, are the currents and locations of the coils. However, in this case, the space for RF between the "focusing" coils is limited.

Another method is to use pancake shaped focus coils. The two parameters are the currents and outer radii of these pancacakes. Adequate space for the RF can be obtained and there is the added advantage that the RF has no coils outside it. But the peak fields in this design are higher, and the ampere turns much higher (up to a factor of 3).

The chosen solution is thus to use a separate "coupling" coil outside the RF, and power it independently of the "focusing" coils at the ends. This arrangement has the big advantage that the two parameters are just the two currents, and the betas can be varied, and the symmetry maintained, by adjusting these currents without changing the physical design. This done here, first with a 2.75 m long lattice, and then with a 1.65 m one. Three different sets of currents have been specified for each of the lattices, giving a total of six different central β's. If desired, the number of different currents could be further increased to make the change of parameters even more adiabatic, but this will not change the physical designs.

Specific coil dimensions, current densities and fields they generate are given below, but it should be understood that the exact shape of the fields is not important provided that the approximate locations and magnitudes of the end fields, and the approximate magnitude of the central fields are achieved.

The axial fields along the full cooling channel are shown below. The field and periodicity changes can clearly be seen.

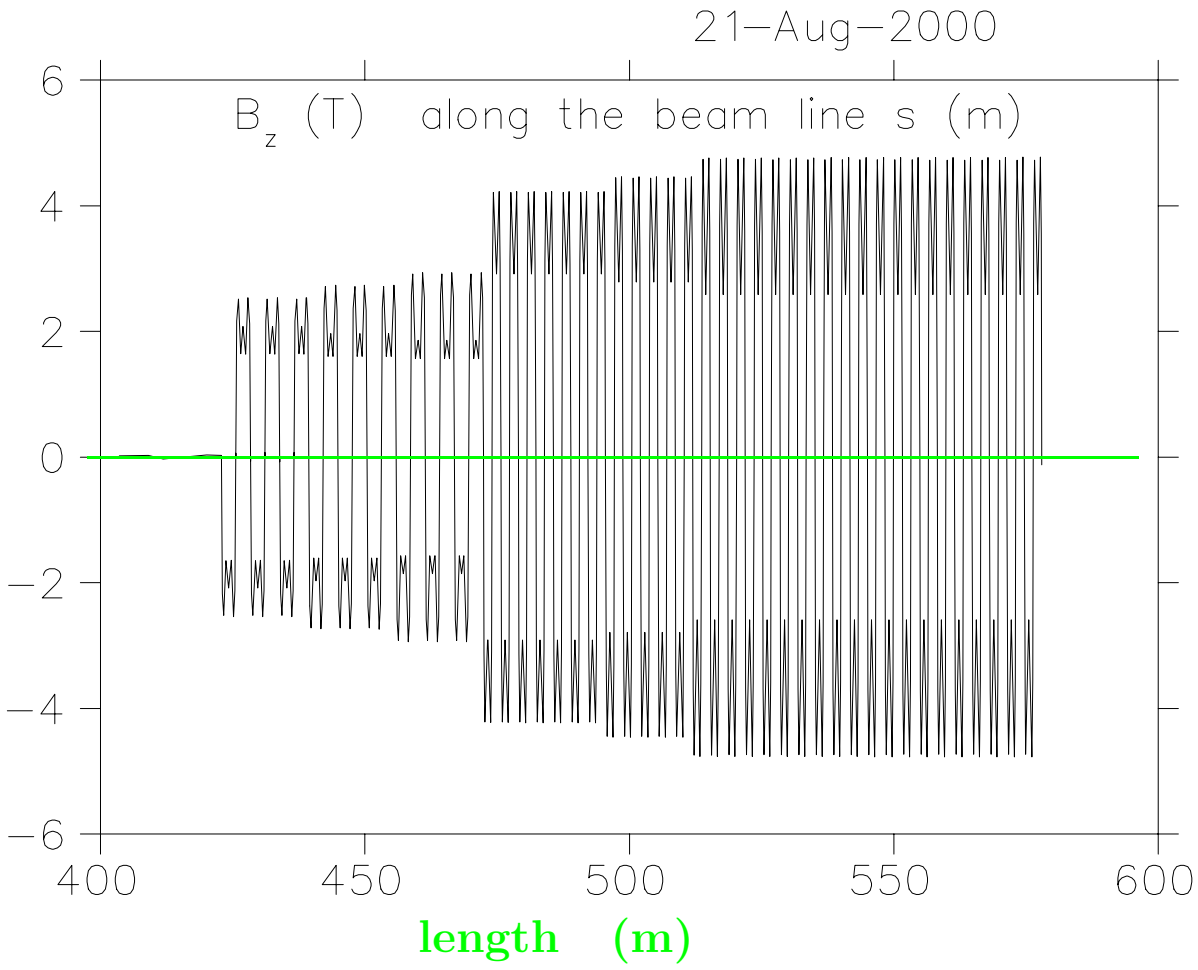

B_z fields along the beam line (T)

2.7.2 Coil dimensions and fields

For the 2.75 m cells:

len1 m	dl m	rad m	dr m	j(1,1)	j(1,2) A/mm^2	j(1,3)
0.175	0.167	0.330	0.175	75.96	84.17	91.46
1.210	0.330	0.770	0.080	99.24	92.42	84.75
2.408	0.167	0.330	0.175	75.96	84.17	91.46

For the 1.65 m cells:

len1 m	dl m	rad m	dr m	j(2,1)	j(2,2) A/mm^2	j(2,3)
0.066	0.145	0.198	0.330	68.76	75.01	83.35
0.627	0.396	0.792	0.099	95.50	87.86	76.40
1.439	0.145	0.198	0.330	68.76	75.01	83.35

2.8 Matching

2.8.1 between sections with same cell length

In all cases a matching section is inserted consisting of two cells: the first as in previous cells, the second as following cells, except that the currents in the central pair of focus coils are set to an average of the currents in the previous and following focus coils.

For instance, for the match from 1,1 to 1,2:

len1 m	gap m	dl m	rad m	dr m	I/A A/mm^2
last 1,1					
0.175	0.175	0.167	0.330	0.175	75.96
1.210	0.868	0.330	0.770	0.080	99.24
2.408	0.868	0.167	0.330	0.175	75.96
match					
2.925	0.175	0.167	0.330	0.175	-75.96
3.960	0.868	0.330	0.770	0.080	-99.24
5.158	0.868	0.167	0.330	0.175	-80.07
5.675	0.175	0.167	0.330	0.175	80.07
6.710	0.868	0.330	0.770	0.080	92.42
7.908	0.868	0.167	0.330	0.175	84.17
first 1,2					
8.425	0.175	0.167	0.330	0.175	-84.17
9.460	0.868	0.330	0.770	0.080	-92.42
10.658	0.868	0.167	0.330	0.175	-84.17

2.8.2 between cells of different lengths (1,3 to 2,1)

len1 m	gap m	dl m	rad m	dr m	I/A A/mm^2	n I A	n I l A m
last 1,3							
2.925	0.175	0.167	0.330	0.175	92.39	2.70	7.08
3.960	0.868	0.330	0.770	0.080	85.61	2.26	11.50
5.158	0.868	0.167	0.330	0.175	92.39	2.70	7.08
match							
5.675	0.175	0.167	0.330	0.175	-92.39	2.70	7.08
6.710	0.868	0.330	0.770	0.080	-85.61	2.26	11.50
7.893	0.853	0.198	0.330	0.175	-95.24	3.30	8.66
8.316	0.066	0.145	0.198	0.330	56.35	2.70	6.16
8.877	0.416	0.396	0.792	0.099	95.65	3.75	19.83
9.689	0.416	0.145	0.198	0.330	68.87	3.30	7.53
first 2,1							
9.966	0.066	0.145	0.198	0.330	-68.87	3.30	7.53
10.527	0.416	0.396	0.792	0.099	-95.65	3.75	19.83
11.339	0.416	0.145	0.198	0.330	-68.87	3.30	7.53

match 1,3 to 2,1

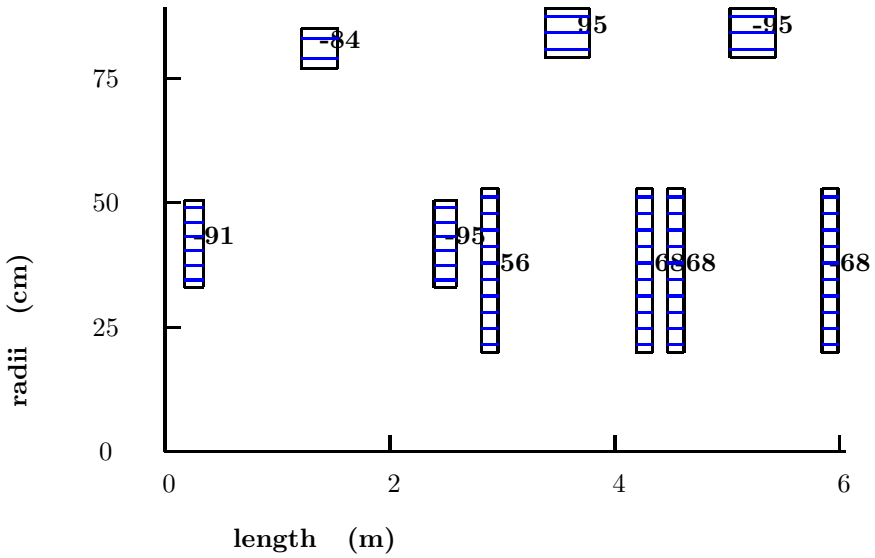

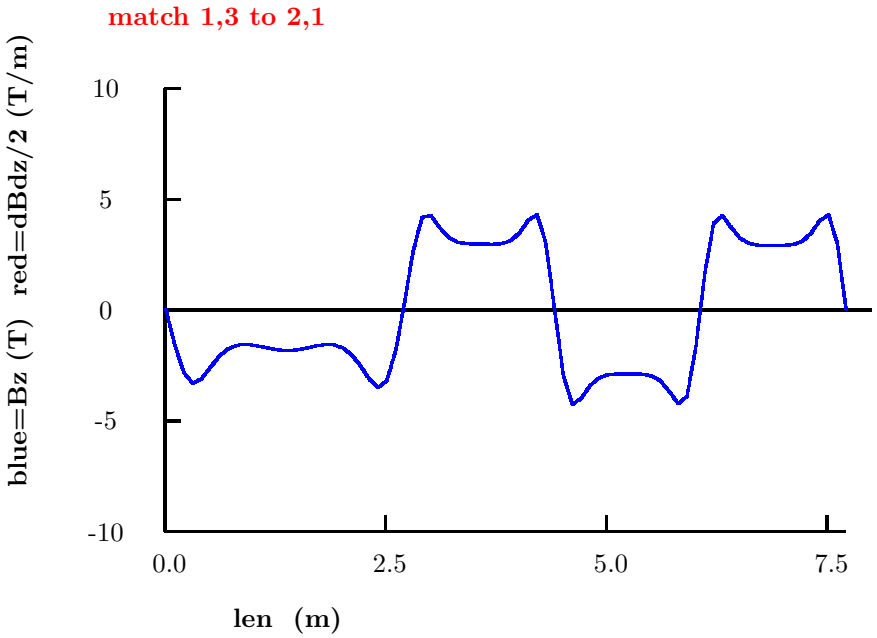
match 1,3 to 2,1
blue=Bz (T) red=dBdz/2 (T/m)
10
5
0
-5
-10
0.0
2.5
5.0
7.5
len (m)

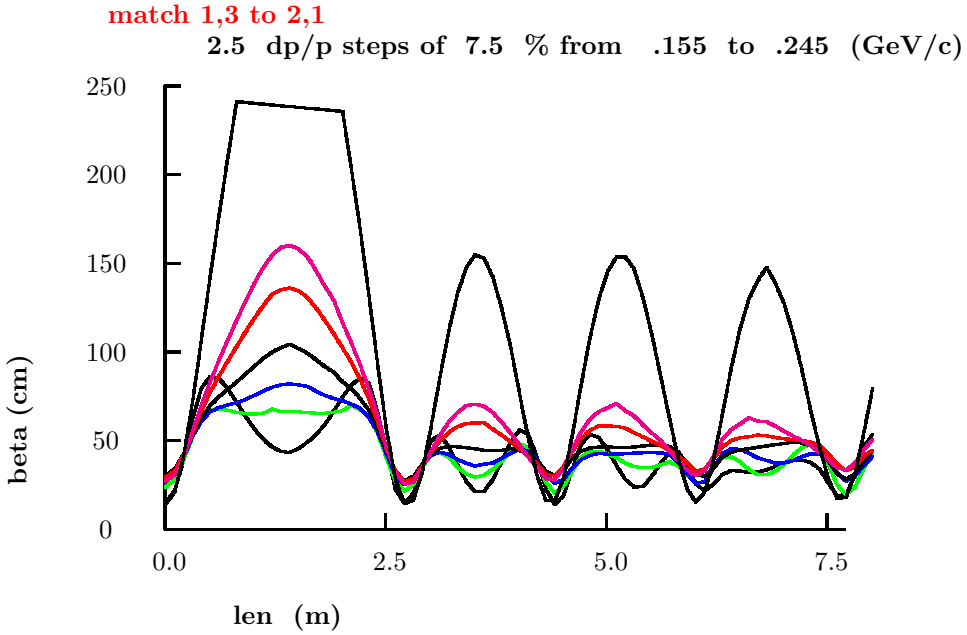
match 1,3 to 2,1
2.5 dp/p steps of 7.5 % from .155 to .245 (GeV/c)
beta (cm)
250
200
150
100
50
0
0.0
2.5
5.0
7.5
len (m)

2.9 Cooling RF

The hydrogen absorbers and rf within the three 2.75 m (or 1.65 m) lattices are all the same except for their apertures which will be given in a separate table.

2.9.1 2.75 m lattices

	dl cm	gradient MV/m	phase deg
Hydrogen	35/2		
Space	26.7		
RF	4 × 46.6	15.48	40
Space	26.7		
Hydrogen	35/2		

2.9.2 Match from 1,3 to 2,1

Note that there is no hydrogen in the center of the match and that the phases are adjusted to correct for the resulting lack of energy loss.

	dl cm	gradient MV/m	phase deg
Hydrogen	35/2		
Space	26.7		
RF	4 × 46.6	15.48	18.8
Space	70.6		
RF	2 × 55.9	16.72	18.8
Space	16		
Hydrogen	21/2		

2.9.3 1.65 m lattices

	dl cm	gradient MV/m	phase deg
Hydrogen	21/2		
Space	16		
RF	2 × 55.9	16.72	40
Space	16		
Hydrogen	21/2		

2.10 Hydrogen Windows

sec	H2		
	t	r	mat
	μm	cm	
1,1-3	360	18	Al
2,1-3	220	11	Al

2.11 RF Windows in Stepped Be Foil

RF Windows

Sec	ends					center				
	t2	t1	r1	r2	mat	t2	t1	r1	r2	mat
	μm	μm	cm	cm		μm	μm	cm	cm	
1,1-3	400	200	12	18	Be	1400	700	14	21	Be
Match 1,3 to 2,1	400	200	12	18	Be	1400	700	14	21	Be
2,1-3	200	100	10	15	Be	760	380	12	18	Be

ALTERNATIVE: Grid of tubes

An alternative to the edge cooled Be foils considered above, FNAL has suggested a grid of gas cooled Al pipes. There are known field problems if the pipes have large diameters, but these must be reduced as their diameteters are reduced and their numbers increase. A second advantage of many small tubes is that, for a given pressure, their wall thicknesses can be reduced. One would like $\leq$ 1 cm diameter pipes, spaced on centers = 2 $\times$ their diameter, with wall thicknesses of $\leq$ 1 mill (25 μm). With 1 atmosphere of gas in the pipes, the tension in the walls would be 3000 psi which should be ok.

sec	r	t	cover	layers
	cm	μm	%	
1,1-1,3	30	25	50	2
2,1-2,3	25	25	50	2

The grid is simulated by foils with thickness equal to the average thickness of the pipes: 80 microns.

2.12 Acceleration

The requirements for the acceleration system are:

initial momentum	210	MeV/c
final energy	20	GeV
Transverse acceptance	15	mm rad
Longitudinal acceptance	150	mm
bunch spacing	201.25	MHz
number of bunches	67	
total muons per bunch train	3	10^{13}

The number of muons specified correspond to a 1.5 MW driver and 0.2 μ's/p.

2.13 Storage Ring

To Carlsbad	2903	km
Dip angle	13.1	deg
Dip angle	.229	rad
Bearing	267.45	deg
Tunnel diam	10	ft
Cover	20	ft
Burm angle	27	deg
Arc Rad	16.9	m
Water table	45	ft
Decay len / circ	35	%

decay/circ %	circ. m	decay m	len m	dh m	hill m	vol yrd^3
35	332	116	148	34	30	225k

Alternative to Soudan

To Soudan	1713	km
Dip angle	7.73	deg
Dip angle	.134	rad
Bearing	303.33	deg
Decay len / circ	40	%

decay/circ %	circ. m	decay m	len m	dh m	hill m	vol yrd^3
40	550	220	252	34	30	250k